Molecules and Cells

Gut Microbial Metabolites Induce Changes in Circadian Oscillation of Clock Gene Expression in the Mouse Embryonic Fibroblasts

Kyojin Ku, Inah Park, Doyeon Kim, Jeongah Kim, Sangwon Jang, Mijung Choi, Han Kyoung Choe, and Kyungjin Kim*

Department of Brain and Cognitive Sciences, Daegu Gyeongbuk Institute of Science and Technology (DGIST), Daegu 42988, Korea
*Correspondence: kyungjin@dgist.ac.kr
https://doi.org/10.14348/molcells.2020.2309
www.molcells.org

Circadian rhythm is an endogenous oscillation of about 24-h period in many physiological processes and behaviors. This daily oscillation is maintained by the molecular clock machinery with transcriptional-translational feedback loops mediated by clock genes including *Period2* (*Per2*) and *Bmal1*. Recently, it was revealed that gut microbiome exerts a significant impact on the circadian physiology and behavior of its host; however, the mechanism through which it regulates the molecular clock has remained elusive. 3-(4-hydroxyphenyl)propionic acid (4-OH-PPA) and 3-phenylpropionic acid (PPA) are major metabolites exclusively produced by *Clostridium sporogenes* and may function as unique chemical messengers communicating with its host. In the present study, we examined if two *C. sporogenes*-derived metabolites can modulate the oscillation of mammalian molecular clock. Interestingly, 4-OH-PPA and PPA increased the amplitude of both PER2 and *Bmal1* oscillation in a dose-dependent manner following their administration immediately after the nadir or the peak of their rhythm. The phase of PER2 oscillation responded differently depending on the mode of administration of the metabolites. In addition, using an organotypic slice culture *ex vivo*, treatment with 4-OH-PPA increased the amplitude and lengthened the period of PER2 oscillation in the suprachiasmatic nucleus and other tissues. In summary, two *C. sporogenes*-derived metabolites are involved in the regulation of circadian oscillation of *Per2* and *Bmal1* clock genes in the host's peripheral and central clock machineries.

Keywords: 3-(4-hydroxyphenyl)propionic acid, 3-phenylpropionic acid, *Bmal1*, circadian rhythm, gut microbiome, *Per2*, real-time bioluminescence recording

INTRODUCTION

Circadian rhythm displays endogenous oscillation of approximately 24-h period in various biological processes. This rhythm is entrained by diverse environmental cues such as light/dark cycle and fluctuation of temperature (Rensing and Ruoff, 2002; Wright et al., 2013). By coordinating the external time cue, organisms are able to maintain normal physiology and behavior at the appropriate time of the day. Even without the external cues, the internal clock can maintain the circadian rhythm per se. In mammals, the master clock residing in the suprachiasmatic nucleus (SCN) of the anterior hypothalamus serves as the central peacemaker and synchronizes the peripheral clocks through humoral and neuronal cues (Honma, 2018).

The mammalian molecular clock network consists of two loops, namely core and auxiliary (or stabilizing) loops. In the core loop, the positive elements, circadian locomotor output

Received 10 December, 2019; revised 31 January, 2020; accepted 10 February, 2020; published online 10 March, 2020

eISSN: 0219-1032

cycles kaput (CLOCK) and brain and muscle arnt-like protein-1 (BMAL1), heterodimerize and initiate the transcription of target genes including *Periods (Per)*, *Cryptochromes (Cry)*, *Rev-erbα, RORα*, and clock-controlled genes (CCGs) by acting on the E-boxes in their promoter regions. The heterodimer of PERIOD (PER) and CRYPTOCHROME (CRY) gives negative feedback to CLOCK and BMAL1 heterodimer complex and represses their own transcription. In the auxiliary loop, REV-ERVα and retinoic acid receptor-related orphan receptor α (RORα) regulate ROR/REV-ERB response elements (ROREs) in the *Bmal1* promoter region. RORα positively regulates the transcription of *Bmal1*, while REV-ERVα negatively controls it respectively (Takahashi, 2017). This molecular time-keeping system is necessary for the maintenance of the circadian rhythms of physiological and neural functions (Refinetti, 2016).

Recently, compelling evidence indicates that gut microbiota plays an important role in controlling the development, physiology, and behaviors of the host (Cryan and Dinan, 2012; Kim et al., 2017; Sgritta et al., 2019). Gut microbiota is defined as an ecological community of symbiotic and pathogenic microorganisms in the gastrointestinal tract (Bäckhed et al., 2005). In fact, gut microbiota produces a variety of metabolic compounds related to neurotransmitters and signaling molecules that may influence physiological consequences including the circadian rhythm of the host (Ge et al., 2017; Leone et al., 2015; Parkar et al., 2019). For instance, circadian oscillation of *Bmal1* transcript in the small intestine of antibiotics-induced microbiota depleted mice was down-regulated by the dysbiosis of gut microbiota (Mukherji et al., 2013) and the circadian pattern of *Per2* mRNA expression in the hepatic organoid changed upon treatment with various metabolites from gut microbiota (Leone et al., 2015). These results strongly suggest that gut microbiota can influence the host circadian rhythm.

It is of note that small chemical compounds exclusively produced by gut microbiota could act as chemical messengers and influence the physiological regulation of the host. Gut microbiota digests dietary carbohydrates, thereby producing many compounds that cannot be broken down by the host metabolism (Jones, 2014; Makki et al., 2018). Interestingly, the genus *Clostridium*, one of the major microbiomes in the gut microbiota, produces a unique set of metabolites to achieve chemical communication with the host (Liang and Fitzgerald, 2017; Thaiss et al., 2014). Among their metabolites, the biochemical pathways of three metabolites, 4-hydroxyl-phenylpropionic acid (4-OH-PPA) and phenylpropionic acid (PPA) are recently identified to be exclusively produced by *Clostridium sporogenes* (Dodd et al., 2017; Elsden et al., 1976). We presumed that *C. sporogenes*-derived metabolites, 4-OH-PPA and PPA, could affect physiological functions such as the circadian rhythm of the host. To test this hypoth-

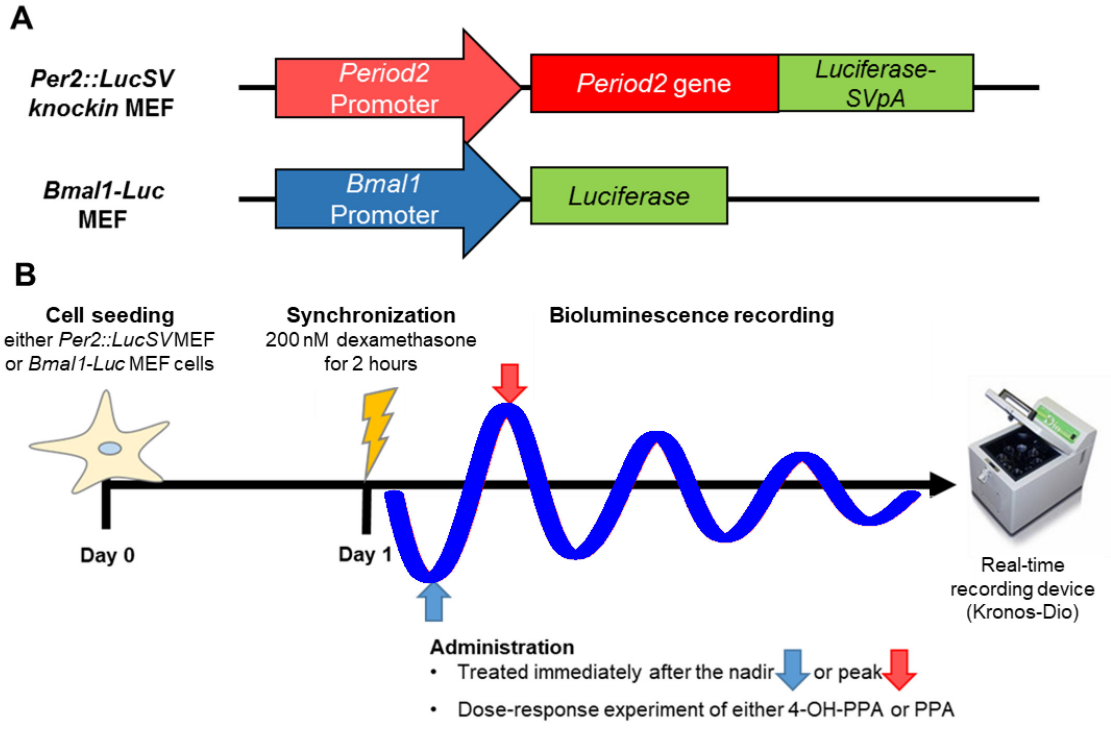

Fig. 1. Experimental scheme for profiling *Per2* and *Bmal1* circadian oscillation following the administration of two metabolites derived from *C. sporogenes* using real-time bioluminescence recording. (A) In *Per2::LucSV* knockin MEF, PER2 protein fused with luciferase was expressed under the control of *Per2* promoter and in *Bmal1-Luc* MEF, luciferase was expressed under the control of *Bmal1* promoter. (B) A schematic diagram to investigate the effect of *C. sporogenes*-derived metabolites *in vitro*. Cells were seeded 1 day prior to 200 nM dexamethasone treatment (a synchronization signal of circadian clock). 4-OH-PPA or PPA was administered at two different circadian points, either immediately after the first nadir or the first peak after synchronization as indicated.

esis, the effect of 4-OH-PPA and PPA on the expression of circadian clock genes in genetically engineered mouse embryonic fibroblast (MEF) cell lines expressing luciferase (Luc) reporter under the control of *Per2* gene and *Bmal1* promoter was examined using a real-time bioluminescence monitoring technique. The effect of 4-OH-PPA on PER2 oscillation profiles in several neural and peripheral tissues derived from *Per2::Luc* knockin mouse was also examined.

MATERIALS AND METHODS

Cell culture

MEF cells were generated from *Per2::LucSV* knockin (Yoo et al., 2017) and *Bmal1-Luc* (Nakajima et al., 2010) transgenic mice. In *Per2::LucSV* knockin MEF cells, luciferase fused with endogenous PER2 protein was expressed, and in *Bmal1-Luc* MEF cells, the expression of luciferase was under the control of *Bmal1* promoter (Fig. 1A). MEF cells were incubated in the CO_2 incubator (Thermo Fisher Scientific, USA) at 37°C and 5% CO_2. The cells were cultured in Dulbecco's modified Eagle's medium (Gibco, USA) supplemented with 10% fetal bovine serum (Gibco) and 1% Antibiotic-Antimycotic (Gibco). Cells were subcultured at 80% confluence once every 2 days.

Real-time recording of circadian gene-regulated bioluminescence *in vitro*

Real-time bioluminescence recording was conducted according to a previously described method with minor modification (Lee et al., 2016). A day before the real-time recording, MEF cells were seeded in 35 mm dish (Fisher Scientific, USA) at 50% confluence. After 24 h, culture media was changed to synchronization media with 200 nM dexamethasone (Sigma-Aldrich, USA) to synchronize circadian rhythms of cell population (So et al., 2009) for 2 h. To record the real-time bioluminescence, synchronized cells were cultured in recording media with 200 μM D-luciferin (Promega, USA) and culture dishes were sealed with parafilm (Sigma-Aldrich). Next, the dishes were placed in Kronos, a real-time bioluminescence recording device (ATTO, Japan), at 37°C and 5% CO_2, and luciferase (Luc) activity in each dish was measured for 1 min every 10 min for 3 to 5 days. For the dose-response effect of 4-OH-PPA and PPA, the cells were treated with four different doses, 0.125 mM, 0.5 mM, 1 mM, and 2 mM of 4-OH-PPA (Sigma-Aldrich) and PPA (Sigma-Aldrich) using two different administration modes, either immediately after the nadir or the peak of the oscillation (Fig. 1B). To verify the effect of 4-OH-PPA and PPA, their precursors, tyrosine (Sigma-Aldrich) and phenylalanine (Sigma-Aldrich), were examined initially as the control experiments.

Animal care and organotypic slice culture

Per2::Luc knockin mice (Yoo et al., 2004) were maintained in a specific pathogen free (SPF) condition at 23°C under 12:12 light/dark cycle with standard mouse chow and water. All animal procedures were approved by the Institutional Animal Care and Use Committee of laboratory animal resource center in Daegu Gyeongbuk Institute of Science and Technology (DGIST-IACUC-19070201-01). Organotypic culture was prepared by Stoppini method (Stoppini et al., 1991) with minor modifications. Briefly, heterozygous *Per2::Luc* neonatal mice between postnatal days 5 to 7 were anesthetized on ice and several tissues were removed for culture. The excised brain was coronally sectioned at a thickness of 400 μm using the VT1000S vibratome (Leica Biosystem, Germany), and the SCN and hippocampus were used in this experiment. Peripheral tissues including liver and small intestine were trimmed and placed onto the culture insert (Merck, Germany) in a 24 well plate (SPL Life Sciences, Korea) with pre-warmed culture media (minimal essential media [MEM] supplemented with 25% horse serum [Gibco], 25% Gey's balanced salt solution [Sigma-Aldrich], 36 mM glucose and 100 U/ml Antibiotic-Antimycotic). The cultures were incubated at 37°C and 5% CO_2. Next day, the slice culture media were replaced and during stabilization for 2 weeks, the slice culture media were replaced once every 3 days.

For real-time bioluminescence recording *ex vivo*, a method previously described by Koo et al. (2015) was used. After the preparation, the tissue was cultured in synchronization media with 1 μM final concentration of dexamethasone for 2 h except for the SCN. After 2 h of synchronization, the tissue was transferred to pre-warmed recording media (culture media containing 200 μM D-Luc). The dishes were sealed with parafilm and placed in Kronos device as described above.

Statistical analysis

The analysis of circadian rhythm after the administration of metabolites or vehicle was performed using FFT-NLLS function from the online BioDare2 analysis platform (https://www.biodare2.ed.ac.uk) (Zielinski et al., 2014). Three peaks of PER2 circadian expression and a single peak of *Bmal1* circadian expression after administration of drug was used for analysis. The change (Δ) in the amplitude and period of respective oscillatory cycles of *Per2* and *Bmal1* genes was defined as a relative difference based on the control values. Statistical significance in the period and amplitude of real-time bioluminescence data was evaluated by one-way ANOVA followed by *post hoc* Dunnett's test. On the other hand, the significance of phase response was additionally calculated by two-way ANOVA followed by *post hoc* Bonferroni's test to compare the effects of the different modes of administration (nadir vs peak). *Ex vivo* real-time bioluminescence data were analyzed by unpaired two-tailed Student's *t*-test. Experiments were replicated at least 4 to 6 times, and the data on the amplitude and period of clock gene oscillation profiles are presented as mean ± SEM. A P value < 0.05 indicated statistical significance.

RESULTS

Effects of 4-OH-PPA and PPA on real-time oscillation profiles of PER2 and *Bmal1* circadian gene expression *in vitro*

To investigate if *C. sporogenes*-derived two metabolites, 4-OH-PPA and PPA, can affect the circadian profiles of clock gene expression, we used a real-time bioluminescence recording method to monitor PER2 expression in the *Per2::LucSV* knockin MEF cells (Yoo et al., 2017). As the biochemical pathways synthesizing 4-OH-PPA and PPA in *C.*

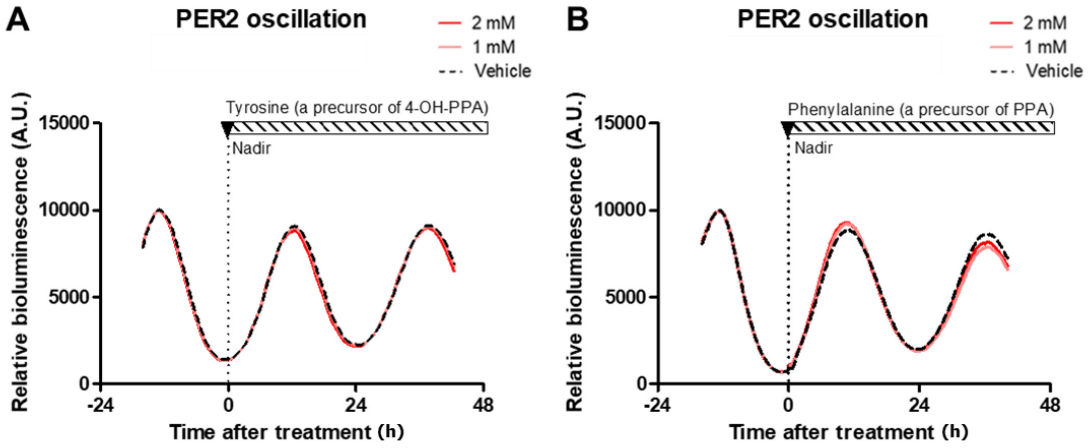

Fig. 2. Precursors of *C. sporogenes*-derived metabolites did not alter PER2 oscillation. The precursor molecules, either tyrosine as a precursor of 4-OH-PPA (A) and phenylalanine as a precursor of PPA (B), had no effect on PER2 oscillation, following their administration immediately after the first nadir. PER2 oscillation is represented with a dotted line (vehicle) and red-colored line (precursor molecules). The point of continuous administration is indicated at the upper side of the graphs (Experiments are repeated n = 4 times for vehicle and n = 6 times for each dose of tyrosine or phenylalanine treatment).

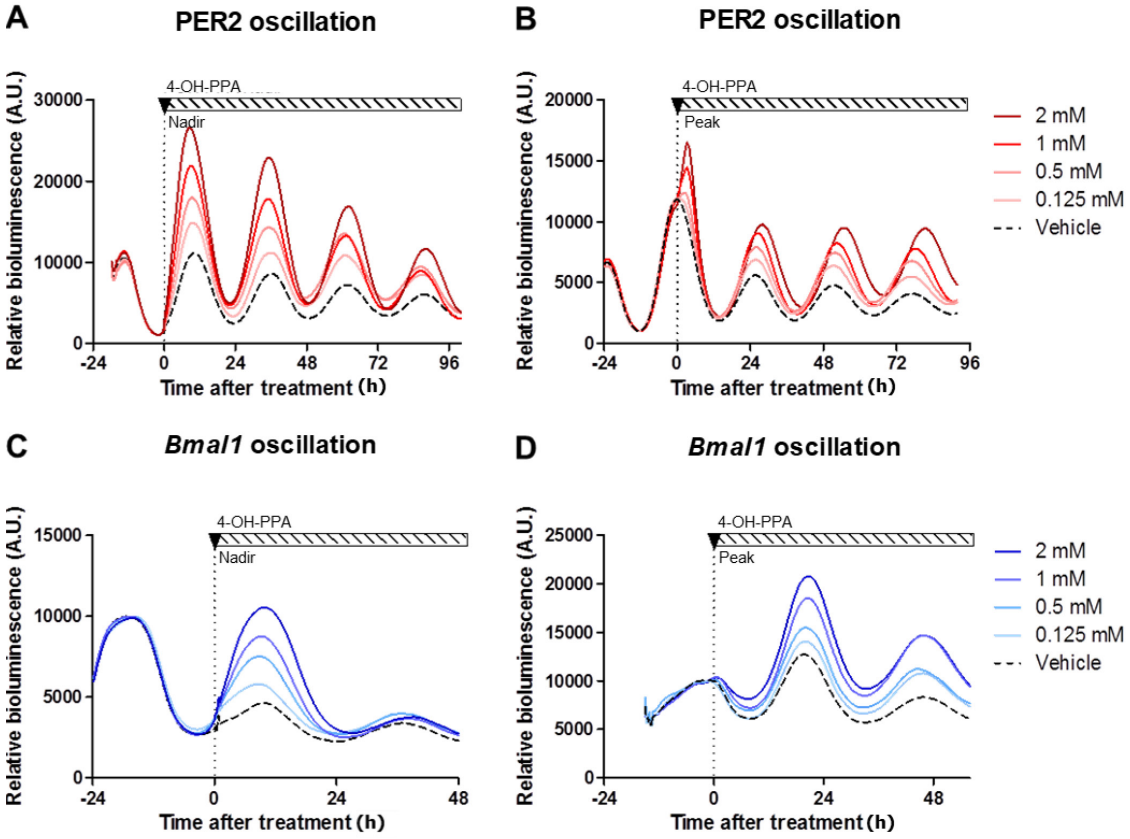

Fig. 3. Dose-response of PER2 and *Bmal1* oscillations induced by the administration of 4-OH-PPA either at nadir or peak. (A and B) Real-time bioluminescence recording of PER2 oscillation in response to 4-OH-PPA at four different doses (0.125, 0.5, 1, and 2 mM) using *Per2::LucSV* knockin MEF cultured *in vitro*. 4-OH-PPA was administered either immediately after the nadir (A) or at the peak (B) of PER2 oscillation. The mode of administration of 4-OH-PPA is indicated at the upper side of the graphs (Experiments are replicated n = 8 times for vehicle and n = 6 times for each dose of 4-OH-PPA-treated group). (C and D) Real-time bioluminescence recording of *Bmal1* oscillation in response to 4-OH-PPA with four different doses (0.125, 0.5, 1, and 2 mM) using *Bmal1-Luc* MEF cultured *in vitro*. 4-OH-PPA was administered either immediately after the nadir (C) or at the peak (D) of *Bmal1* oscillation (Experiments are replicated n = 8 times for vehicle and n = 6 times for each dose of 4-OH-PPA treatment).

sporogenes were recently characterized (Dodd et al., 2017), identifying tyrosine and phenylalanine as the precursors of 4-OH-PPA and PPA, respectively. Therefore, we initially conducted control experiments using the precursors of the metabolites. As shown in Fig. 2, these two amino acids did not alter PER2 oscillation. Furthermore, we examined the effect of 4-OH-PPA and PPA on PER2 oscillation at four different doses (0.125 mM, 0.5 mM, 1 mM, and 2 mM). Because organisms change internal status under the control of circadian rhythm and may react differently, we adopted two different administration modes, either immediately after the nadir or the peak of circadian oscillation. 4-OH-PPA increased the amplitude of PER2 circadian expression in a dose-dependent manner regardless of the administration modes (Figs. 3A and 3B). The changes (Δ) in period and amplitude of four consecutive cycles were calculated based on the value of vehicle group (Table 1). Higher doses of 4-OH-PPA increased the period significantly except when 1 mM 4-OH-PPA was treated immediately after the peak of PER2 oscillation. The circadian oscillation of PER2 expression showed higher amplitude in the 4-OH-PPA treatment groups when compared with vehicle groups in both nadir and peak administration modes (Table 1).

We also determined *Bmal1* circadian expression by applying real-time bioluminescence recording technique to MEF derived from *Bmal1-Luc* mice (Nakajima et al., 2010). The amplitude of *Bmal1* circadian rhythm was increased by the four different doses of 4-OH-PPA at the first circadian oscillation and damped at the second cycle (Figs. 3C and 3D). Even though the period was not affected at any of the doses of 4-OH-PPA on *Bmal1* oscillation, 4-OH-PPA significantly increased the amplitude of *Bmal1* oscillation at the higher

Table 1. Changes in period and amplitude of circadian oscillation after 4-OH-PPA treatment

	Dosage (mM)	Treatment mode			
		Nadir		Peak	
		Period (Δ)	Amplitude (Δ)	Period (Δ)	Amplitude (Δ)
PER2 oscillation with administration of 4-OH-PPA	0	1.000 ± 0.002	1.000 ± 0.020	1.000 ± 0.003	1.000 ± 0.022
	0.125	0.998 ± 0.002	1.270 ± 0.090	0.987 ± 0.005	1.302 ± 0.026***
	0.5	1.003 ± 0.004	1.668 ± 0.110***	0.987 ± 0.006	1.628 ± 0.019***
	1	1.009 ± 0.003*	1.904 ± 0.142***	1.005 ± 0.004	2.095 ± 0.025***
	2	1.041 ± 0.002***	2.724 ± 0.096***	1.030 ± 0.007***	2.298 ± 0.111***
Bmal1 oscillation with administration of 4-OH-PPA	0	1.000 ± 0.012	1.000 ± 0.085	1.000 ± 0.012	1.000 ± 0.123
	0.125	1.039 ± 0.061	1.421 ± 0.165	1.012 ± 0.030	1.153 ± 0.131
	0.5	1.043 ± 0.049	2.294 ± 0.269**	1.009 ± 0.012	1.364 ± 0.184
	1	1.086 ± 0.031	2.929 ± 0.274***	1.011 ± 0.014	2.080 ± 0.257**
	2	1.108 ± 0.011	3.794 ± 0.462***	1.035 ± 0.011	2.416 ± 0.265***

Data are presented as mean ± SEM. In either PER2 or *Bmal1* oscillation, experiments are replicated n = 8 times for vehicle; n = 6 times for each dose of 4-OH-PPA treatment. Statistical significance was assessed by one-way ANOVA followed by *post hoc* Dunnett's test, $*P < 0.05$, $**P < 0.01$, and $***P < 0.001$ compared with the vehicle group.

Table 2. Changes in period and amplitude of circadian oscillation after PPA treatment

	Dosage (mM)	Treatment mode			
		Nadir		Peak	
		Period (Δ)	Amplitude (Δ)	Period (Δ)	Amplitude (Δ)
PER2 oscillation with administration of PPA	0	1.000 ± 0.002	1.000 ± 0.014	1.000 ± 0.002	1.000 ± 0.018
	0.125	1.002 ± 0.005	1.159 ± 0.033*	0.999 ± 0.002	1.255 ± 0.026***
	0.5	1.005 ± 0.002	1.253 ± 0.038***	1.004 ± 0.003	1.381 ± 0.022***
	1	1.021 ± 0.004***	1.520 ± 0.045***	1.025 ± 0.001***	1.627 ± 0.032***
	2	1.043 ± 0.002***	1.883 ± 0.080***	1.039 ± 0.003***	1.770 ± 0.025***
Bmal1 oscillation with administration of PPA	0	1.000 ± 0.008	1.000 ± 0.081	1.000 ± 0.019	1.000 ± 0.070
	0.125	1.099 ± 0.044	1.154 ± 0.127	1.027 ± 0.005	1.085 ± 0.037
	0.5	1.076 ± 0.071	1.459 ± 0.210	1.015 ± 0.014	1.153 ± 0.056
	1	1.066 ± 0.037	2.056 ± 0.236**	0.965 ± 0.010	1.694 ± 0.053***
	2	1.154 ± 0.075*	2.695 ± 0.367***	1.002 ± 0.013	1.852 ± 0.046***

Data are presented as the mean ± SEM. In PER2 oscillation, experiments are repeated n = 8 times for vehicle; n = 6 times for each dose of 4-OH-PPA treated group and in *Bmal1* oscillation, n = 6 times for vehicle; n = 6 times for each dose of 4-OH-PPA. Statistical significance was assessed by one-way ANOVA followed by *post hoc* Dunnett's test, $*P < 0.05$, $**P < 0.01$, and $***P < 0.001$ compared with the vehicle group.

doses (1 mM and 2 mM) (Table 1).

Similar to 4-OH-PPA, the period of PER2 circadian expression was lengthened by the higher doses (1 mM and 2 mM) of PPA at both nadir and peak of its oscillation. However, the period of *Bmal1* rhythmicity was significantly lengthened only with the administration of 2 mM PPA immediately after the nadir due to more damping at the second peak. In addition, the administration of PPA at the four different doses increased the amplitude of PER2 and *Bmal1* oscillation in a dose-dependent manner (Table 2, Fig. 4). The increase in amplitude was greater with 4-OH-PPA than with PPA (Please compare Tables 1 and 2).

We also examined the phase shift of PER2 oscillation induced by 4-OH-PPA and PPA with the two administration modes. Depending on the mode of administration, 4-OH-PPA (Fig. 5A) and PPA (Fig. 5B) revealed different phase shifts in a dose-dependent manner. The peak phase of PER2 oscillation was delayed with treatment administered immediately after the nadir, whereas the peak phase was advanced with treatment administered immediately after the peak.

Effect of 4-OH-PPA on circadian oscillation of PER2 in organotypic cultures *ex vivo*

According to the *in vitro* results, the 4-OH-PPA caused greater alterations in PER2 oscillation when compared with PPA treatment, especially at the peak time point. We proceeded to examine if 4-OH-PPA can affect PER2 circadian oscillation *ex vivo*. We used four different tissue regions derived from *Per2::Luc* knockin mice: the SCN containing the master clock, hippocampus (one of the brain local clocks), liver, and small intestine (two other peripheral clocks). In comparison with the vehicle, 4-OH-PPA at 2 mM increased PER2 oscillation in the SCN tissue when administered at the peak, resulting in higher amplitude and lengthened period of PER2 oscillation (Fig. 6A). In the hippocampus, 4-OH-PPA treatment elicited a significant increase in the amplitude, but not the period of PER2 (Fig. 6B). In the two peripheral tissues (liver and small intestine), 4-OH-PPA treatment significantly increased the amplitude and lengthened the period of PER2 oscillation (Figs. 6C and 6D). These *ex vivo* results demonstrated that the rhythmicity of PER2 circadian oscillation consistently en-

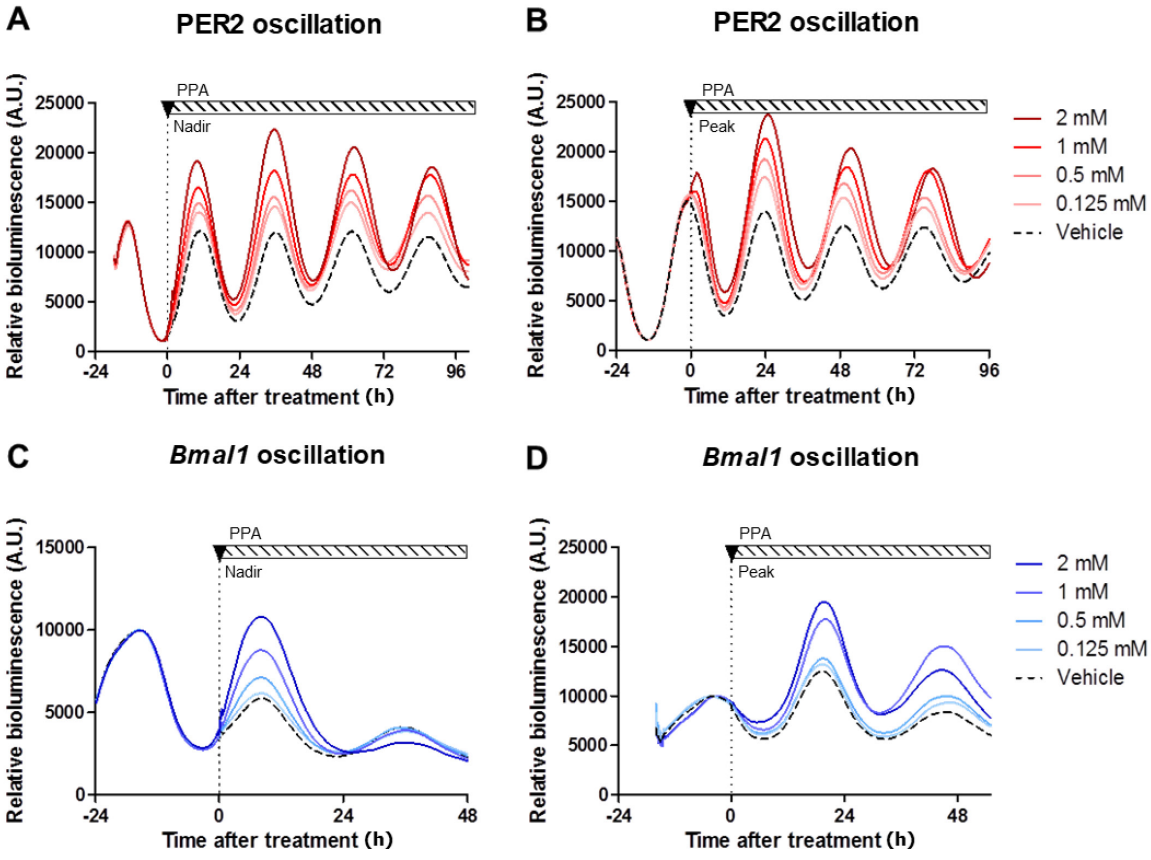

Fig. 4. Dose-response of PER2 and *Bmal1* oscillations induced by PPA administered either at nadir or peak. (A and B) Real-time bioluminescence recording of PER2 oscillation in response to PPA at four different doses (0.125, 0.5, 1, and 2 mM) using *Per2::LucSV* knockin MEF cultured *in vitro*. 4-OH-PPA was administered either immediately after the nadir (A) or the peak (B) of PER2 oscillation. The mode of administration of PPA is indicated at the upper side of the graphs (Experiments are replicated n = 8 times for vehicle and n = 6 times for each dose of PPA-treated group). (C and D) Real-time bioluminescence recording of *Bmal1* oscillation in response to PPA at four different doses (0.125, 0.5, 1, and 2 mM) using *Bmal1-Luc* MEF cultured *in vitro*. PPA was administered either immediately after the nadir (C) or the peak (D) of *Bmal1* oscillation (Experiments are replicated n = 6 times for vehicle and n = 6 times for each dose of PPA treatment).

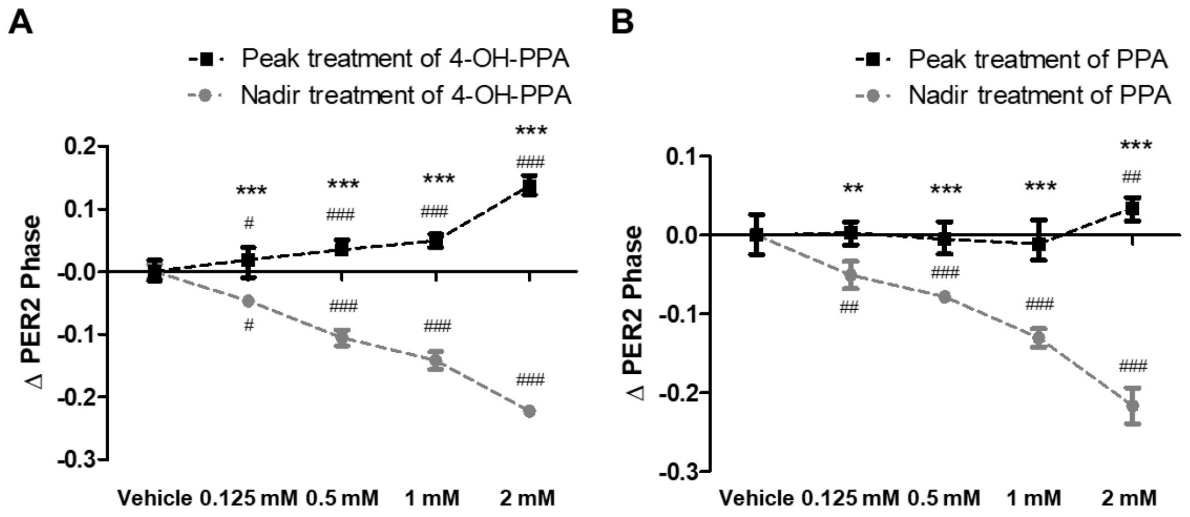

Fig. 5. Phase response of *Period2* oscillation when two metabolites, 4-OH-PPA and PPA, were administered either at nadir or peak. (A and B) Phase shift with advance and delay data are presented as the mean ± SEM. The relative changes (Δ) between control and experimental groups (Experiments are replicated n = 8 times for vehicle and n = 6 times for each dose of 4-OH-PPA or PPA treated group). Phase response of PER2 oscillation by the administration of four different doses of 4-OH-PPA (A) or PPA (B). Depending on the administration mode, data are expressed at peak (black dotted line) and nadir (gray dotted line). Statistical significance in each group was evaluated by one-way ANOVA followed by *post hoc* Dunnett's test, $^{\#}P < 0.05$, $^{\#\#}P < 0.01$, and $^{\#\#\#}P < 0.001$ vs vehicle-treated group. To compare the effects of the different administration modes (nadir and peak), the statistical significance of phase changes was assessed by two-way ANOVA followed by *post hoc* Bonferroni's test, $^{**}P < 0.01$ and $^{***}P < 0.001$.

hanced the amplitude in the four tissue regions examined. Increased amplitude was accompanied by the increased overall expression of PER2::LUC in the brain oscillators, the SCN and hippocampus, but not in the peripheral oscillators, the liver and small intestine. The increased amplitude in the peripheral oscillators was due to the difference in the bioluminescence of the peak and the nadir rather than the increase of basal bioluminescence throughout the oscillation. It appeared that 4-OH-PPA exhibited a tissue-specific modulation of the circadian rhythm of each tissue.

DISCUSSION

In the present study, we demonstrated that two metabolites of *C. sporogenes*, 4-OH-PPA and PPA, regulated the circadian oscillation of *Per2* and *Bmal1* genes in the MEF cells. First, 4-OH-PPA and PPA increased the amplitude of both PER2 and *Bmal1* oscillation in a dose-dependent manner with a significant increase at higher concentrations (1 mM and 2 mM). The period of PER2 oscillation was lengthened by 4-OH-PPA and PPA, and the phase response in PER2 circadian oscillation differed significantly depending on the mode of treatment. In addition, the organotypic cultures of the SCN, hippocampus, liver, and small intestine derived from *Per2::Luc* knockin mice revealed that the effect of 4-OH-PPA on circadian rhythm in the MEF cells can be reproduced at the tissue level to a certain extent. In fact, 2 mM 4-OH-PPA affected the circadian rhythm of all of the tissue regions by increasing the amplitude and lengthening the period of PER2 oscillation.

The dosage of metabolites used in the present study (0.125-2 mM) was within the physiological range because endogenous concentrations of 4-OH-PPA and PPA in human blood are around 0.5 mM according to human metabolome database (Wishart et al., 2018). It appears that metabolites produced by *C. sporogenes* can affect the host's molecular circadian clock at a physiologically relevant level.

Even though gut microbiota is not directly exposed to external time cues, such as light/darkness cycle, it has been known that gut microbiota including clostridium exhibits diurnal fluctuation that is influenced by feeding rhythms and metabolic profiles over the course of time of the day, are revealed recently by gut microbiome studies (Liang and Fitzgerald, 2017; Thaiss et al., 2014). In addition, antibiotics treatment disturbed the compositional changes in gut microbiota leading to physiological consequences such as gut motility (Ge et al., 2017). Considering the daily fluctuation in the concentration of metabolites produced by *Clostridium*, it is important to assess circadian profiles depending on the different responses to circadian time points. As shown in Fig. 5, the two modes of administration (nadir and peak) of the drugs yielded different phase shift of circadian oscillation in the MEF cells. The phase shift is important because it can determine when to exert certain physiology correctly by advance or delay (Eastman et al., 2015). In fact, it has been known that short-chain fatty acid (SCFA), one of the gut microbial metabolites, and dietary fiber-containing diets regulate the phase of the host's circadian rhythm in the peripheral tissues (Tahara et al., 2018).

The overall robustness of PER2 oscillation pattern in the SCN as a master clock appears to be similar to those of the local clocks in other tissues examined. Throughout the recording, the brain oscillators showed increased average bio-

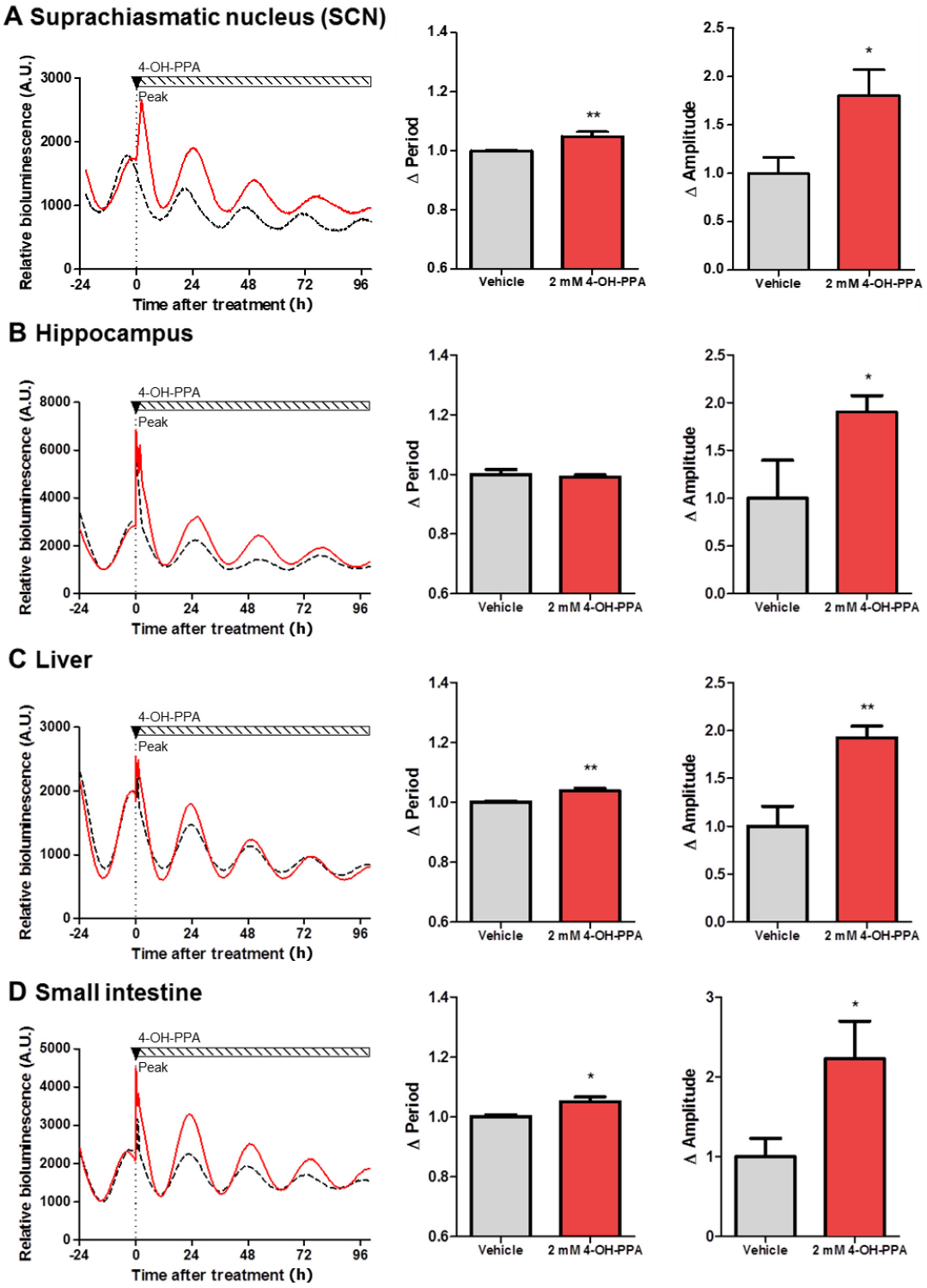

Fig. 6. Period2 oscillation patterns in various tissues cultured *ex vivo* under the administration of 2 mM 4-OH-PPA immediately after the peak. Real-time bioluminescence recording of PER2 oscillation in response to 4-OH-PPA using several tissues cultured *ex vivo*—SCN (A), hippocampus (B), liver (C), and small intestine (D)—from *Per2::Luc* knockin mice. 2 mM 4-OH-PPA or vehicle (MEM) was administered immediately after the peak of PER2 oscillation. The Δ period and Δ amplitude of PER2 circadian expression in each tissue are presented as the mean ± SEM of relative changes between control and experimental group (Experiments are replicated in the SCN, n = 7 times for vehicle, n = 6 times for 2 mM 4-OH-PPA; in the hippocampus, n = 3 times for vehicle, n = 6 times for 2 mM 4-OH-PPA; in the liver n = 8 times for vehicle, n = 8 times for 2 mM 4-OH-PPA; in the small intestine n = 4 times for vehicle, n = 6 times for 2 mM 4-OH-PPA). Statistical significance was assessed by unpaired two-tailed Student's *t*-test, $*P < 0.05$ and $**P < 0.01$ compared with the vehicle.

luminescence with higher basal level after the administration of 4-OH-PPA. However, the peripheral oscillators had the tendency to maintain or lower the basal level. It appeared that there might be differential tissue-specificity in the central and peripheral clock machineries, and this is consistent with the tissue-specific robustness of circadian oscillation repeatedly noticed in the central and local clocks (Buhr et al., 2010; Yoo et al., 2004). Furthermore, it is worth noting that the gut-produced metabolites of *C. sporogenes* may be uptaken into either the blood circulation or the nerve terminals of the nerve system (Abot et al., 2018; Krishnan et al., 2015), transported either into the peripheral tissues or central nervous system (CNS), and involved in the homeostatic regulation of neural functions. Although there is not much information about 4-OH-PPA and PPA, recent researches have been conducted on which receptors are involved to transfer the signal of several representative molecules from the gut microbiota, such as SCFAs (Chen et al., 2019; Lund et al., 2018). Following signaling cascades of these receptors, we may find a clue to figure out how 4-OH-PPA and PPA control expression of circadian genes. Since several papers recently report that the signals from gut microbiota are transferred to the brain through the vagus nerve system (Bonaz et al., 2018; Sgritta et al., 2019), a study using vagotomy would be worthwhile to investigate the physiological significance of *C. sporogenes*-derived metabolites. Thus, further studies are needed to elucidate the mechanism of action in the microbiota-gut-brain axis.

In conclusion, the present study demonstrated that novel function of 4-OH-PPA and PPA produced by *C. sporogenes* playing an important role in modulating the circadian clock machinery in the peripheral tissues.

Disclosure

The authors have no potential conflicts of interest to disclose.

ACKNOWLEDGMENTS

This work was supported by the Ministry of Science, ICT and Future Planning through the National Research Foundation of Korea (NRF-2017R1A2A1A05001351) and DGIST Start-up Fund Program (2019010078).

ORCID

Kyojin Ku https://orcid.org/0000-0002-0996-5816
Doyeon Kim https://orcid.org/0000-0002-9215-7296
Han Kyoung Choe https://orcid.org/0000-0001-7849-7094
Kyungjin Kim https://orcid.org/0000-0002-7128-7374

REFERENCES

Abot, A., Cani, P.D., and Knauf, C. (2018). Impact of Intestinal peptides on the enteric nervous system: novel approaches to control glucose metabolism and food intake. Front. Endocrinol. *9*, 323.

Bäckhed, F., Ley, R.E., Sonnenburg, J.L., Peterson, D.A., and Gordon, J.I. (2005). Host-bacterial mutualism in the human intestine. Science *307*, 1915-1920.

Bonaz, B., Bazin, T., and Pellissier, S. (2018). The vagus nerve at the interface of microbiota-gut-brain axis. Front. Neurosci. *12*, 49.

Buhr, E.D., Yoo, S.H., and Takahasi, J.S. (2010). Temperature as a universal resetting cue for mammalian circadian oscillators. Science *330*, 379-385.

Chen, H., New, P.K., Rosen, C.E., Bielecka, A.A., Kuchroo, M., Cline, G.W., Kruse, A.C., Ring, A.M., Crawford, J.M., and Palm, N.W. (2019). A forward chemical genetic screen reveals gut microbiota metabolites that modulates host physiology. Cell *177*, 1217-1231.

Cryan, J.F. and Dinan, T.G. (2012). Mind-altering microorganisms: the impact of gut microbiota on brain and behavior. Nat. Rev. Neurosci. *13*, 701-712.

Dodd, D., Spitzer, M., Van Treuren, W., Merrill, B., Hryckowian, A., and Higginbottom, S. (2017). A gut bacterial pathway metabolizes aromatic amino acids into nine circulating metabolites. Nature *551*, 648-652.

Eastman, C.R., Suh, C., Tomaka, V.A., and Crowley, S.J. (2015). Circadian rhythm phase shifts and endogenous free-running circadian period differ between African-Americans and European-Americans. Sci. Rep. *5*, 8381.

Elsden, S.R., Hilton, M.G., and Waller, J.M. (1976). The end products of the metabolism of aromatic amino acids by Clostridia. Arch. Microbiol. *107*, 283-288.

Ge, X., Ding, C., Zhao, W., Xu, L., Tian, H., Gong, J., Zhu, M., Li, J., and Li, N. (2017). Antibiotics-induced depletion of mice microbiota induces changes in host serotonin biosynthesis and intestinal motility. J. Transl. Med. *15*, 1-9.

Honma, S. (2018). The mammalian circadian system: a hierarchical multi-oscillator structure for generating circadian rhythm. J. Physiol. Sci. *68*, 207-219.

Jones, M.J. (2014). CODEX-aligned dietary fiber definitions help to bridge the 'fiber gap'. Nutr. J. *13*, 34.

Kim, S., Kim, H., Yim, Y.S., Ha, S., Atarashi, K., Tan, T.G., Longman, R.S., Honda, K., Littman, D.R., Choi, G.B., et al. (2017). Maternal gut bacteria promote neurodevelopmental abnormalities in mouse offspring. Nature *549*, 528-532.

Koo, J., Choe, H.K., Kim, H.D., Chun, S.K., Son, G.H., and Kim, K. (2015). Effect of mefloquine, a gap junction blocker, on circadian period2 gene oscillation in the mouse suprachiasmatic nucleus ex vivo. Endocrinol. Metab. *30*, 361-370.

Krishnan, S., Alden, N., and Lee, K. (2015). Pathways and functions of gut microbiota metabolism impacting host physiology. Curr. Opin. Biotechnol. *36*, 137-145.

Lee, J., Lee, S., Chung, S., Park, N., Son, G.H., An, H., Jang, J., Chang, D.H., Suh, Y.G., and Kim, K. (2016). Identification of a novel circadian clock modulator controlling BMAL1 expression through a ROR/REV-ERB-response element-dependent mechanism. Biochem. Biophys. Res. Commun. *469*, 580-586.

Leone, V., Gibbons, S.M., Martinez, K., Hutchison, A.L., Huang, E.Y., Cham, C.M., Pierre, J.F., Heneghan, A.F., Nadimpalli, A., Hubert, N., et al. (2015). Effects of diurnal variation of gut microbes and high-fat feeding on host circadian clock function and metabolism. Cell Host Microbe *17*, 681-689.

Liang, X. and Fitzgerald, G.A. (2017). Timing the microbes: the circadian rhythm of gut microbiome. J. Biol. Rhythms. *32*, 505-515.

Lund, M.L., Egerod, K.L., Engelstoft, M.S., Dmytriyeva, O., Theodorsson, E., Patel, B.A., and Schwarts, T.W. (2018). Enterochromaffin 5-HT cells - a major target for GLP-1 and gut microbial metabolites. Mol. Metab. *11*, 70-83.

Makki, K., Deehan, E.C., Walter, J., and Bäckhed, F. (2018). The impact of dietary fiber on gut microbiota in host health and disease. Cell Host Microbe *23*, 705-715.

Mukherji, A., Kobiita, A., Ye, T., and Chambon, P. (2013). Homeostasis in intestinal epithelium is orchestrated by the circadian clock and microbiota cues transduced by TLRs. Cell *153*, 812-827.

Nakajima, Y., Yamazaki, T., Nishii, S., Noguchi, T., Hoshino, H., Niwa, K., Viviani, V.R., and Ohmiya, Y. (2010). Enhanced beetle luciferase for high-resolution bioluminescence imaging. PLoS One *5*, e10011.

Parkar, S.G., Kalsbeek, A., and Cheeseman, J.F. (2019). Potential role for the gut microbiota in modulating host circadian rhythms and metabolic health. Microorganisms *7*, E41.

Refinetti, R. (2016). Circadian Physiology (Florida: CRC Press).

Rensing, L. and Ruoff, P. (2002). Temperature effect on entrainment, phase shifting, and amplitude of circadian clocks and its molecular bases. Chronobio. Int. *19*, 807-864.

Sgritta, M., Dooling, S.W., Buffington, S.A., Momin, E.N., Francis, M.B., Britton, R.A., and Costa-Mattioli, M. (2019). Mechanisms underlying microbial-mediated changes in social behavior in mouse models of autism spectrum disorder. Neuron *101*, 246-259.

So, A.Y., Bernal, T.U., Pillsbury, M.L., Yamamoto, K.R., and Feldman, B.J. (2009). Glucocorticoid regulation of the circadian clock modulates glucose homeostasis. Proc. Natl. Acad. Sci. U. S. A. *106*, 17582-17587.

Stoppini, L., Buchs, P., and Muller, D. (1991). A simple method for organotypic cultures of nervous tissue. J. Neurosci. Methods *37*, 173-182.

Tahara, Y., Yamazaki, M., Sukigara, H., Motohashi, H., Sasaki, H., Miyakawa, H., Haragu-chi, A., Ikeda, Y., Fukuda, S., and Shibata, S. (2018). Gut microbiota-derived short chain fatty acids induce circadian clock entrainment in mouse peripheral tissue. Sci. Rep. *8*, 1395.

Takahashi, J.S. (2017). Transcriptional architecture of the mammalian circadian clock. Nat. Rev. Genet. *18*, 164-179.

Thaiss, C.A., Zeevi, D., Levy, M., Zilberman-Schapira, G., Suez, J., Tengeler, A., and Elinav, E. (2014). Transkingdom control of microbiota diurnal oscillations promotes metabolic homeostasis. Cell *159*, 514-529.

Wishart, D.S., Feunang, Y.D., Marcu, A., Guo, A.C., Liang, K., Vázquez-Fresno, R., Sajed, T., Johnson, D., Li, C., Karu, N., et al. (2018). HMDB 4.0: the human metabolome database for 2018. Nucleic Acids Res. *4*, D608-D617.

Wright, K.P., Jr., McHill, A.W., Birks, B.R., Griffin, B.R., Rusterholz, T., and Chinoy, E.D. (2013). Entrainment of the human circadian clock to the natural light-dark cycle. Curr. Biol. *23*, 1554-1558.

Yoo, S.H., Kojima, S., Shimomura, K., Koike, N., Buhr, E.D., Furukawa, T., Ko, C.H., Gloston, G., Ayoub, C., Nohara, K., et al. (2017). Period2 3′-UTR and microRNA-24 regulate circadian rhythms by repressing PERIOD2 protein accumulation. Proc. Natl. Acad. Sci. U. S. A. *114*, E8855-E8864.

Yoo, S.H., Yamazaki, S., Lowrey, P.L., Shimomura, K., Ko, C.H., Buhr, E.D., Siepka, S.M., Hong, H.K., Oh, W.J., Yoo, O.J., et al. (2004). PERIOD2::LUCIFERASE real-time reporting of circadian dynamics reveals persistent circadian oscillations in mouse peripheral tissues. Proc. Natl. Acad. Sci. U. S. A. *101*, 5339-5346.

Zielinski, T., Moore, A.M., Troup, E., Halliday, K.J., and Millar, A.J. (2014). Strengths and limitations of period estimation methods for circadian data. PLoS One *9*, e96462.